Influence of stream turbulence intensity and eddy size of the fluctuating pressure forces on a single tube

Norberg, Christoffer; Sundén, Bengt

Published in:
ASME Winter Annual Meeting

1984

INFLUENCE OF STREAM TURBULENCE INTENSITY AND EDDY SIZE ON THE FLUCTUATING PRESSURE FORCES ON A SINGLE TUBE

C. Norberg and B. Sunden
Chalmers University of Technology
Department of Applied Thermo and Fluid Dynamics
Gothenburg, Sweden

ABSTRACT

This paper presents a systematic investigation of the influence of stream turbulence on the pressure forces on a single tube. Grids were used to produce different turbulent flow fields with longitudinal integral scale (eddy size) ranging from 0.1 to 0.5 tube diameters and turbulence intensities ranging from 0.1 to 3.2 %. The measurements were carried out at two Reynolds numbers, $2.7 \cdot 10^4$ and $4.1 \cdot 10^4$, respectively.

Results are presented for the mean and fluctuating pressures including spectral distributions, skewness and flatness factors of the fluctuating pressure. The rms force coefficients were estimated using the phase differences and rms pressure coefficients around the tube.

The results indicate considerable influence of the turbulence intensity but weaker influence of the eddy size and of the Reynolds number.

NOMENCLATURE

C_D = mean drag coefficient
C'_D = rms drag coefficient
C_p = mean pressure coefficient = $(\bar{p} - p_r)/q$
C'_p = rms pressure coefficient = p'/q
D = tube diameter
f = frequency
f_n = natural frequency of pinhole system
f_S = vortex shedding frequency
p_r = reference static pressure
$\bar{p}$ = mean static pressure
p' = rms pressure fluctuation on the tube surface
q = dynamic head = $\rho U^2/2$
Re_D = Reynolds number = UD/ν
S = Strouhal number = $f_S D/U$
Tu = turbulence intensity = u'/U
U = mean velocity
u' = rms velocity fluctuation

α = angle from forward stagnation point
$\Delta\varphi = \varphi(\alpha) - \varphi(-\alpha)$
ζ = damping parameter of pinhole system
Λ = macroscale of velocity fluctuation
λ = microscale (Taylor) of velocity fluctuation
ν = kinematic viscosity
ρ = density
$\varphi(\alpha)$ = phase between reference and $p(\alpha)$

Subscripts

b = base
m = maximum

INTRODUCTION

In the flow through the interstices of a tube bundle of the type used in heat exchangers, very high level of turbulence may be generated. This turbulence causes buffeting of the tubes, and this is one of the mechanisms by which tube vibration is initiated and sustained. When the dominant frequency of the turbulent flow matches the natural frequency of the tube, a considerable transfer of energy may occur leading to significant vibration.

Turbulent buffeting is not always identified as the primary cause of tube damage but it might initiate the tube motion leading to fluid-elastic instability. Also the buffeting may be the cause of long term damage.

An empirical equation for estimation of the dominant frequency for turbulent buffeting has been proposed by Owen [1]. This equation, obtained from investigations with gas flowing across an ideal tube bundle, does however not include any leading turbulence parameter (e.g. turbulence intensity or eddy size). Thus there is a great need for further investigation.

Although earlier investigations have dealt with the effect of incident turbulence fields on the pressure forces on circular cylinders, the influence of the stream turbulence intensity and eddy size (integral scale) has not been fully revealed. The interaction between the incident turbulence and e.g. vortex shedding is not fully understood and thus there is need for additional investigations. For recent reviews, see [2,3].

The overall objective of the present work is to measure the fluctuating pressure on the surfaces of single tubes and tube bundles and to establish adequate correlations relating these forces to the intensity and scale (eddy size) of the turbulence.
Another objective is to study the interaction of the vortex shedding and stream turbulence and the corresponding influence on the vibration characteristics.

The present paper reports results for a single tube and is a brief account of a comprehensive work on the buffeting phenomenon.

EXPERIMENTAL EQUIPMENT AND INSTRUMENTATION

Windtunnel and turbulence generating grids

The experiments were performed in a closed-circuit low-speed windtunnel, see Fig. 1. The dimensions of the working section are 2.9 m (length), 0.5 m (height) and 0.4 m (width). With a honeycomb and two screens in the settling chamber together with a long contraction, the longitudinal turbulence intensity in the working section is less than 0.1 %.

Turbulent flows can be generated by placing grids across the entrance of the working section. In this investigation, three different grids were used. They were all biplanar with square meshes and circular rods, see Table 1.

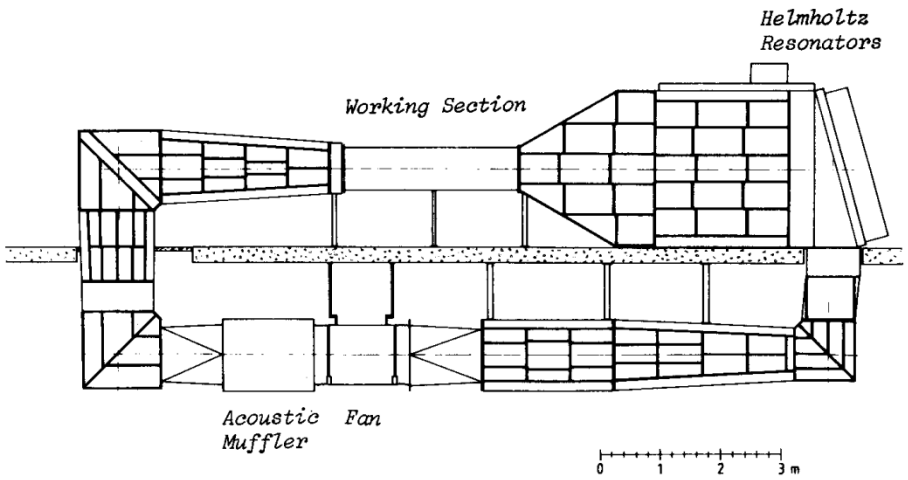

Fig. 1. The windtunnel

Table 1 Data for the turbulence generating grids

Grid No	Bar Size mm	Mesh Size mm	Pressure loss coeff
1	1	5	0.63
2	4	20	0.54
3	7	35	0.56

Velocity field measurements

The measurements of mean and fluctuating velocities upstream the tube were carried out with a Pitot-static tube and single DISA hot wires of 5 µm diameter.

The turbulence structure downstream the grids was at first measured in the empty tunnel. The distributions of the turbulence intensity Tu and the eddy size to diameter ratio Λ/D are shown in Fig. 2.

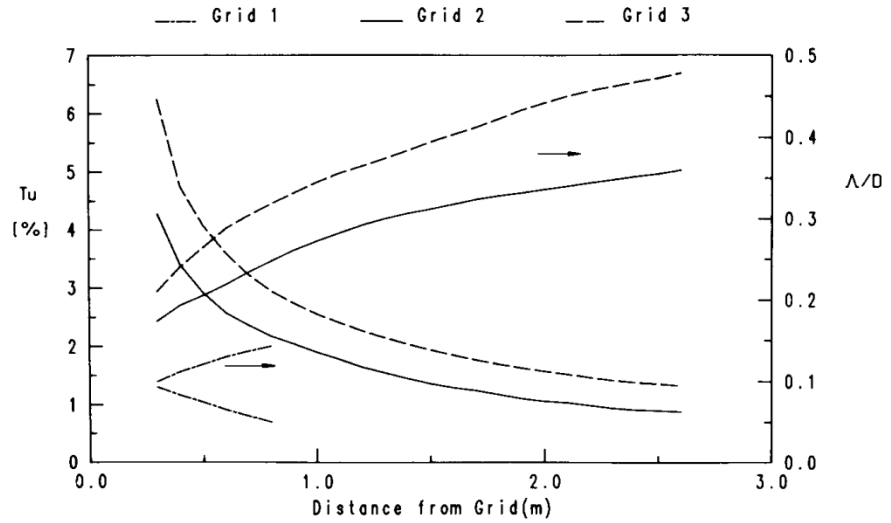

Fig. 2. Turbulence structure downstream the grids

With the tube in place there will be a complex interaction between the mean flow around the tube and the approaching stream turbulence. At some distance upstream the tube, this interaction will be negligible. Typical distributions of the turbulence intensity and the eddy size are depicted in Fig. 3. As is evident, the approaching turbulence undergoes amplification close to the tube surface.

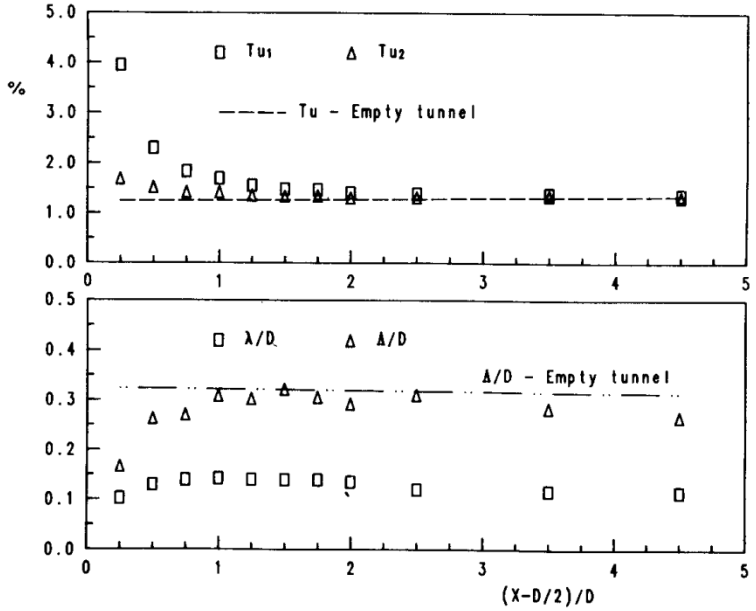

Fig. 3. Turbulent structure in the working section with and without the tube in place. Tu_1 - local Tu, Tu_2 - Tu based on freestream velocity.
Note: X from tube axis, stagnation line.

The position where the turbulence intensity is independent of the presence of the tube can be taken as the definition point for the approaching turbulence. This definition has been used in related heat transfer studies [4-6]. However, in the present work, the definition is taken from the curves in Fig. 2 at the position downstream the grids where the tube is placed during the measurements. The relation between these two methods of definition can be found from Fig. 3.

To enable a systematic variation in the turbulent parameters, the tube was placed at different positions downstream the grids. In that way, the turbulence intensity can be kept constant while the eddy size is varied or alternatively, the eddy size can be kept constant while the intensity is varied.

In these flow measurements, a digital data aquisition system with a VAX 11/750 computer was employed. A sampling frequency of 10 kHz was used and 200 ksamples were taken at each point of measuring. The eddy size (Λ) was obtained as the mean value of the macroscale from the autospectrum (low frequency limit) and the integral time scale using Taylor's hypothesis.

Measurements of the fluctuating pressures on the tube

The tube had an outer diameter of 41 mm and was divided in two sections. One section was a steel pipe while the other was made of aluminium and contained a microphone which was connected to the tube surface through a cannula (pinhole arrangement) which was 9.5 mm long and had an inner diameter of 0.4 mm, see Fig. 4.

In the spanwise direction pressure taps of 0.5 mm, connected to a manometer, were placed. The outer surface of the tube was polished.

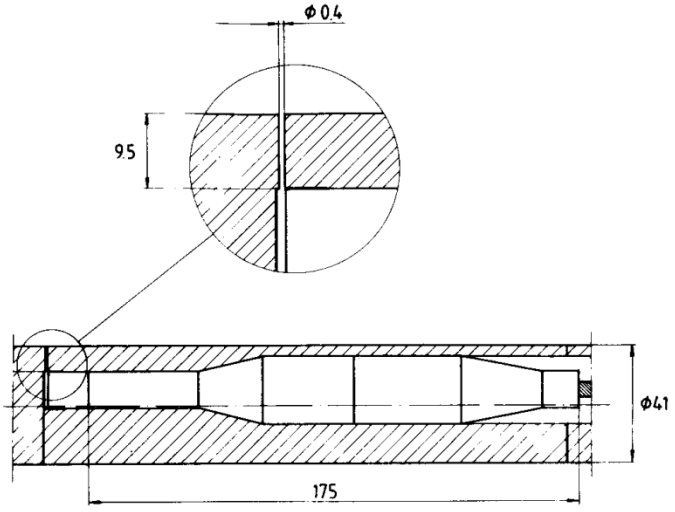

Fig. 4. Test tube with microphone in pinhole arrangement. Dimensions in mm.

The tube was mounted horizontally and rigidly between the side-walls of the working section but could be rotated in steps of 1 deg and positioned at different locations.

In order to obtain a two-dimensional flow around the tube and to obtain correct levels of the measured pressure distribution and the calculated drag coefficient, it was found necessary to use end plates on the tube. To find the proper placement of the end plates, an investigation was carried out. This investigation suggested that if the end plates were placed approximately 35 - 40 mm from the side-walls of the windtunnel (just outside the wall layers) results sufficiently independent of the end plate position were obtained. Similar problems have been investigated and discussed in [7,8]. With the end plates (similar design as in [7,8]) in place, a blockage ratio of 8.3 % and a span length to diameter ratio of 8.0 prevailed.

The acoustic pressure field in the tunnel was measured by microphones flush-mounted in the tunnel floor and by microphones (equipped with nose cones) placed in the stream.

The microphone system employed was of Bruel and Kjaer fabrication (1/2" microphone Type 4147 with Carrier System Type 2631) and had a frequency response ranging from 0.01 Hz to 16 kHz ($\pm$ 1 dB). The sensitivity checked by a Sound Level Calibrator (B & K Type 4230) and the in-built calibration signal was typically 20 mV/Pa.

The frequency response for the pinhole arrangement showed a Helmholtz resonance which could be described as a second-order system (f_n = 635 Hz, ζ = 0.31). The calculated spectral distributions were corrected for this frequency response. The unfiltered output from the pinhole microphone was dominated by frequencies below 250 Hz and therefore it was of secondary importance.

Vibration studies were made with an accelerometer (B & K Type 4368, Conditioning Amplifier Type 2626).

When necessary, the outputs from the transducers were filtered and amplified

(Krohn Hite Model 3340 and 3700). For accurate measurements of the root mean square (rms) and mean voltages a HP Digital Voltmeter 3456A was used.

In the sampling and evaluation of data the VAX 11/750 computer again was used. The sampling frequency and the number of samples taken were chosen in such a way that suitable resolution and high statistical accuracy were achieved. In the spectral analysis the signals were low-pass filtered at half the sampling frequency in order to avoid aliasing errors.

Fluctuating lift and drag forces

The spanwise and circumferential correlations between the fluctuating pressures at two points on the tube surface are of great engineering importance in that they yield information about the rms-values and spanwise coherence of the fluctuating lift and drag forces.

For these correlation measurements we are using a technique similar to the one used by Kiya et al. [9] and Arie et al. [10]. These measurements are not completed but will be reported in a later paper. However, estimations for the fluctuating forces using a simplified procedure will be given.

Disturbances

Acoustic disturbances in a windtunnel may influence the fluctuating flow field and the associated forces on an object placed in the flow but to which extent is not fully revealed, see [11,12].

An extensive study of the acoustic disturbances in our windtunnel showed that the sound level in the working section was high, typically 2 % of the dynamic head at 10 m/s (no grid). Spectral and correlation analysis showed that the major contribution was concentrated in a frequency band around 30 Hz associated with a longitudinal standing acoustic wave. The corresponding wavelength matched with the distance between the corners in the upper part of the tunnel system.

An installation of 17 tuned Helmholtz resonators and an ordinary acoustic muffler reduced the sound level by a factor greater than 2.

Also, the standing wave pattern implies that the associated wave-components at different locations are coherent. By measuring the coherence function between an additional microphone flush-mounted in the tunnel floor far upstream the tube ($\geq$ 10 diameters) and the pinhole microphone it was possible to subtract or compensate for the remaining part of these disturbances.

It is worth noting that on the major part of the tube surface the flow - induced pressure fluctuations are of such a magnitude that the disturbances are negligible. However, in the stagnation zone the fluctuations are small, especially if the oncoming flow is non-turbulent. At this region of the tube surface the subtraction technique was applied.

The use of end plates to reduce the interference effect from the tunnel walls has been described earlier.

Other common types of disturbances present in investigations like this were controlled without any large difficulties.

RESULTS

Results from ten different cases are reported, see Table 2. At first no end plates were fitted to the tube. This resulted in pressure distributions and drag coefficients which for the non-turbulent cases deviated much from the generally accepted values. The cause of this was found to be interference effects from the boundary layers on the tunnel walls. To remedy this, end plates had to be used as outlined in an earlier section.

All cases were in the subcritical range where the flow is dominated by vor-

tex shedding.

Table 2 Parameters for cases investigated. X - Distance downstream the grids, U - Nominal velocity.

Case	Grid No	X[m]	U[m/s]	Tu[%]	Λ/D	λ/D	C_D	S
0	-	1.7	10	0.1	-	-	1.18	0.192
1	-	1.7	15	0.1	-	-	1.21	0.189
2	3	0.7	10	3.25	0.31	0.11	1.26	0.189
12	3	0.7	15	3.15	0.29	0.11	1.25	0.188
4	1	0.3	10	1.30	0.10	0.08	1.21	0.187
11	1	0.3	15	1.33	0.10	0.07	1.22	0.186
3	2	1.7	10	1.28	0.32	0.16	1.26	0.190
8	2	1.7	15	1.26	0.31	0.14	1.26	0.187
7	3	2.6	10	1.34	0.49	0.20	1.20	0.188
10	3	2.6	15	1.28	0.46	0.18	1.20	0.186

Mean quantities

Fig. 5 depicts the mean pressure coefficient for some of the cases in Table 2. Data were corrected for tunnel blockage by the method of Allen and Vincenti as described in [13,14]. The maximum correction applied for the mean velocity and the drag coefficient were 3.4 and 7.9 %, respectively.

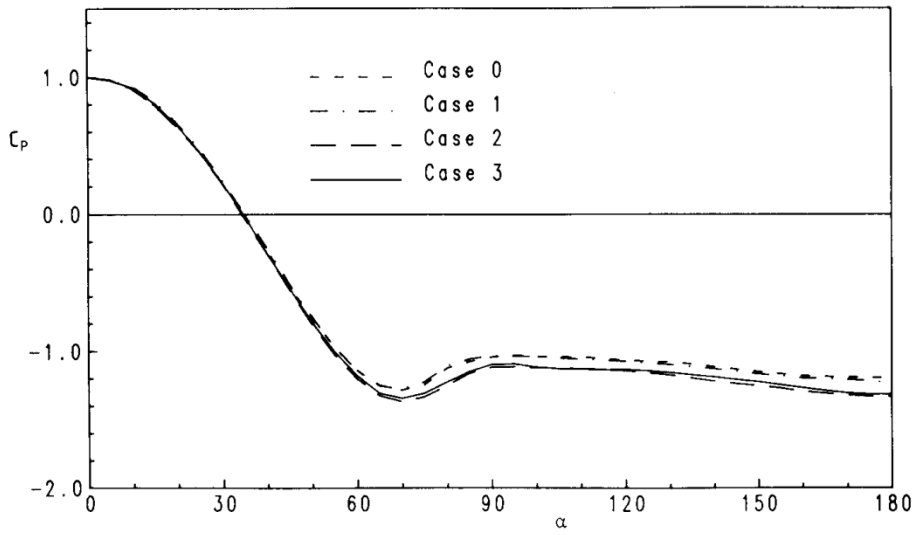

Fig. 5. Distributions of the mean pressure coefficient, $C_p(\alpha)$, on the tube surface. Cases refer to Table 2.

From Fig. 5 it is evident that the mean pressure coefficient on the upstream side of the tube is almost unaffected by the stream turbulence. This is in agreement with the assumptions and findings in [4-6]. The base pressure in the wake region is however slightly altered by the stream turbulence and thus there is an interaction between the external turbulence and the wake flow.

The mean drag coefficients were determined by integration of the mean pressure distributions. The vortex shedding frequencies were determined from spec-

tral measurements at α = 60 deg (resolution $\approx$ 0.2 Hz). Table 2 shows that when the Reynolds number was changed from $2.7 \cdot 10^4$ ($\approx$ 10 m/s) to $4.1 \cdot 10^4$ ($\approx$ 15 m/s) a slight increase in the drag coefficient appeared. The corresponding Strouhal number ($S = f_S D/U$, f_S shedding frequency) decreased slightly (non-turbulent cases). However, these variations were smaller for the turbulent cases. For the non - turbulent cases the values of the mean drag coefficient are in agreement with the standard data reported in e.g. [15]. This confirms that for all cases, the flow is in the pre-transitional range.

RMS - distributions

The distribution of the rms pressure coefficient C'_p are presented in Fig. 6 for the same cases as in Fig. 5.

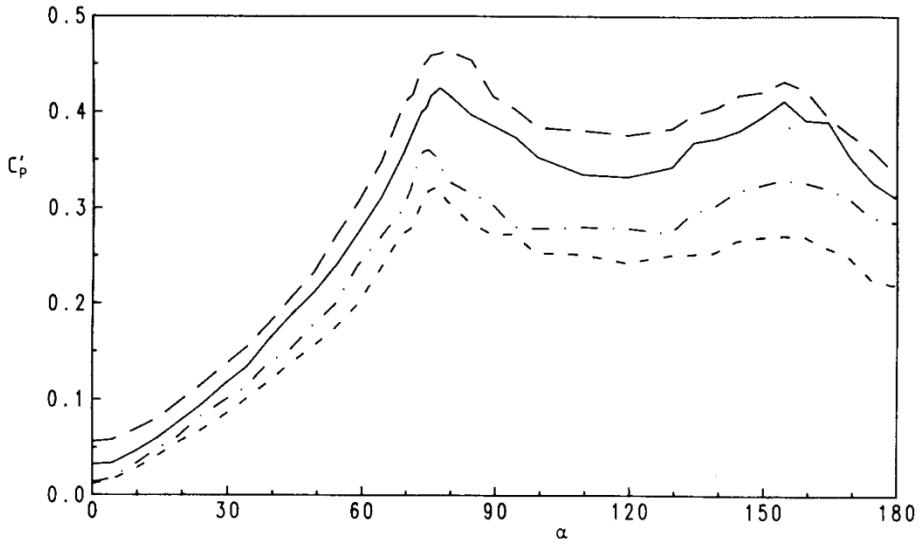

Fig. 6. Distributions of the rms pressure coefficient, $C'_p(\alpha)$, on the tube surface. For legend, see Fig. 5.

All distributions exhibit a maximum at an angle of about 77 deg, which is close to the separation point. The similarity between the distributions is significant. This is in accordance with other investigations, for instance [9,16]. The span in C'_p covered by the different cases clearly demonstrates the sensitivity to variations in the turbulence of the oncoming flow. The Reynolds number effect on C'_p was small except for the non-turbulent flow. The non-turbulent cases are in agreement with i.e. [17].

The rms-pressure fluctuations around the tube are increased by the blockage (see e.g. Modi and El-Sherbiny [18]). The similarity in the C'_p - distributions therefore suggests that an increase in the dynamic head is an appropriate correction to the rms-pressure coefficient. However, this blockage effect is not fully understood and therefore no correction was applied in this investigation.

The maximum value of the rms-pressure coefficient (C'_{p_m}) increased by the stream turbulence by as much as 45 %. The rms-pressure coefficient at the base (C'_{p_b}) is also affected by the turbulence. Changes of order 30 - 50 % occur compared to the non-turbulent flow. Both the turbulence intensity and the integral scale (eddy size) influence these coefficients although the effect of the scale is weaker.

A direct comparison with other studies is not possible since the effect of the turbulence intensity and eddy size have not usually been separated.

Spectral and statistical analysis

When the oncoming flow was turbulent the levels of the pressure fluctuation spectra were increased for all values of α. The angular variation of the power spectral density (PSD) for case 12 (see Table 2) is shown in Fig. 7. The peak at the fundamental Strouhal frequency (f_S) disappears at the rear stagnation point (α = 180 deg) where the energy around the second harmonic ($2f_S$) has a maximum. The component at three times the shedding frequency ($3f_S$) is discernible, in particular between α = 130 - 160 degrees. Except for high frequencies the spectral distributions are similar for all the cases investigated.

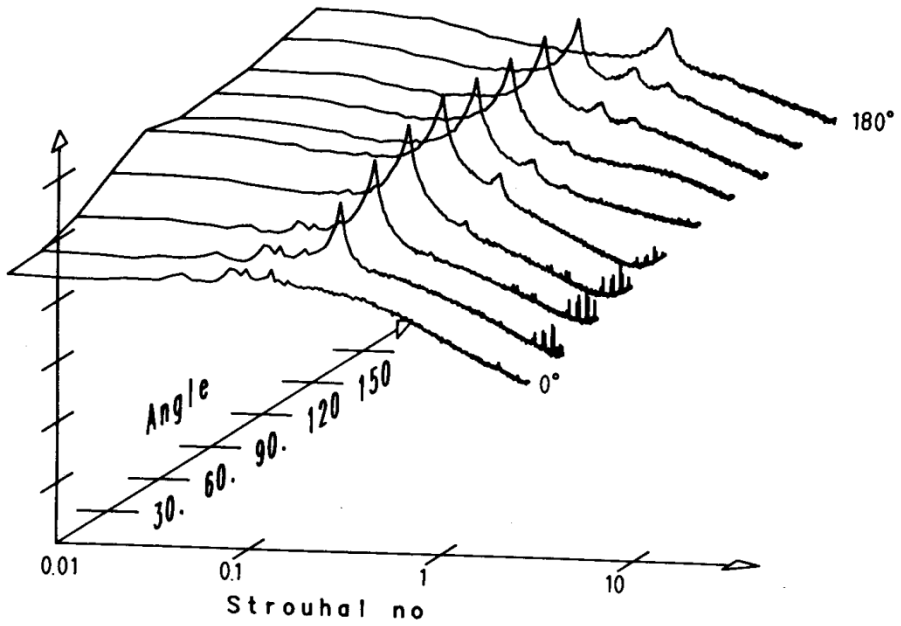

Fig. 7. Power spectral density distribution. Case 12.
Note: 20 dB between ticmarcs on vertical axis.
Strouhal no = fD/U.

The pressure signals showed a strong low-frequency amplitude modulation which increased from the stagnation point. The importance of these modulations was pointed out by Sonneville [19], who suggested that they were associated with slow changes in the region of formation of the shedding.

The distributions in different Strouhal-bands at different positions are shown in Fig. 8 (Case 11, see Table 2).

The energy around the fundamental Strouhal frequency (fD/U = 0.1 - 0.3) dominates the spectra except near the rear region. This level, which is associated with the strength of the vortices shed, was influenced by the turbulence. The half-power (-3 dB) bandwidth was increased by the velocity but the turbulence effect was small.

Further measurements are needed to clarify phase- and coherence-relations for different spectral components.

The statistical analysis was based on computation of the probability density function (PDF) of the pressure signals (statistical moments, minimum and maximum pressures). The distributions in Fig. 9 are typical in a general view for all cases.

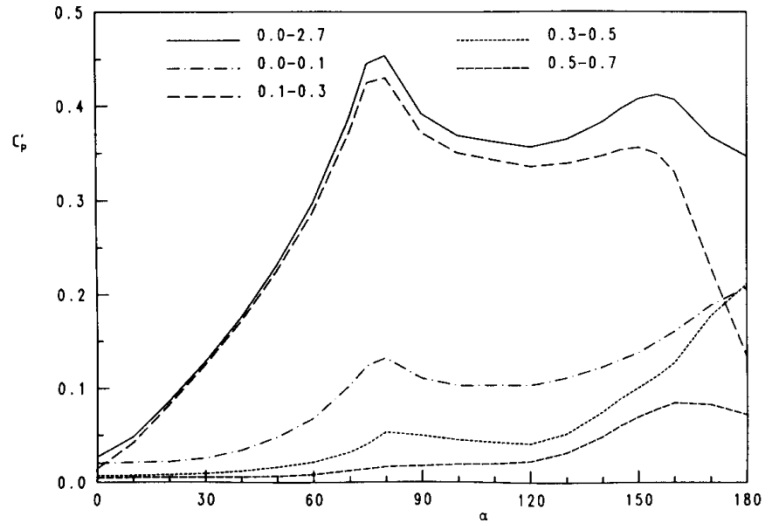

Fig. 8. Distribution of C_p' in different Strouhal-bands around the tube surface. Case 11 (see Table 2).

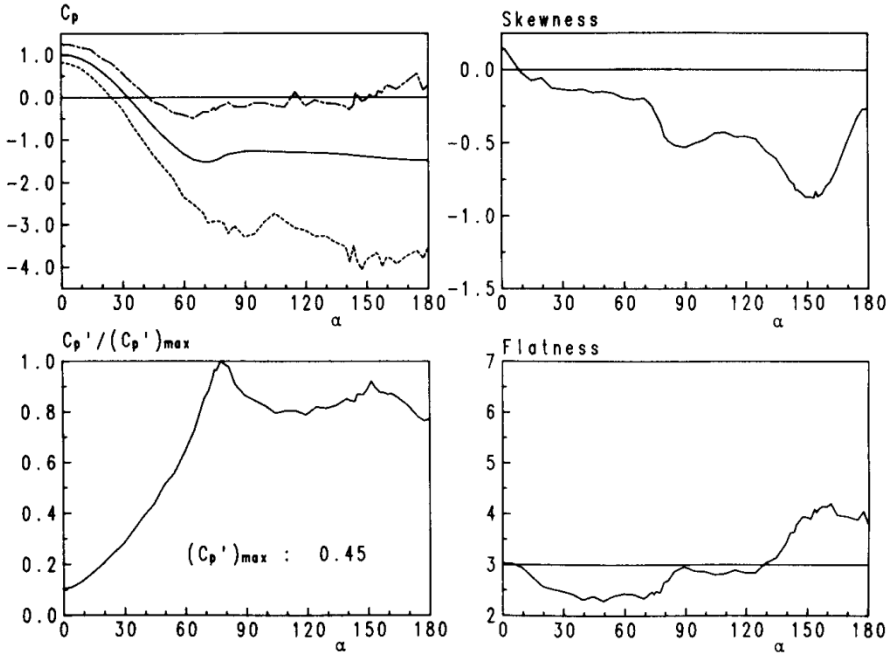

Fig. 9. Statistical moments, minimum and maximum pressures at different positions on the tube surface. Case 12.

On the stagnation line (α = 0 deg) the distributions are almost Gaussian (skewness = 0, flatness = 3) and the amplitude is dependent on the upstream turbulence level. The fluctuations grow in magnitude in the boundary layer region up to the separation point. In the region of decelerated flow (adverse pressure gradient), the minimum pressure coefficient reaches a minimum and the rms-distribution a maximum ($\alpha \approx 77$ deg). The higher order moments change very rapidly in this region. For angles between 90 and 120 degrees, the variations are small. The most striking feature is the variations in the region $\alpha \approx 130 - 160$ degrees. The intermittency of the pressure in this region is reflected in the extreme values of the higher order moments (rms, skewness, flatness). This seems to be associated with the entrainment of fluid bearing vorticity of opposite sign (secondary circulation) discussed by Surry [16] and Gerrard [20].

Estimation of the fluctuating forces

So and Savkar [2] found that for Reynolds numbers between $10^4 - 10^5$, conservative estimates of the fluctuating lift force coefficient C_L' and the fluctuating drag coefficient are obtained by the relations $C_L'/C_D = 0.8$ and $C_D'/C_D = 0.1$, respectively.

The distance between the tube and the place where the periodic wake is formed decreases at a Reynolds number of about $2 \cdot 10^3$ and the wake is formed close to the shoulder (α = 90 deg) at a Reynolds number of about $5 \cdot 10^4$ (non-turbulent flow), see Bloor [21]. The measurements by Gerrard [22,23] show that the flow in this Reynolds number range is highly sensitive to disturbances (e.g. freestream turbulence). He also found that the variations in the rms-pressure coefficient and the turbulence intensity at the shoulder are similar to the variations in C_L'. In another investigation by Kiya et al. [9] it was found that $C_L'/C_p'(90) \approx 2$.

In order to estimate the fluctuating forces on the tube, the phase - difference between the fluctuating velocity 0.1 diameter above the tube at α = 90 deg and the fluctuating pressures around the tube surface was measured (mid-span position). Fig. 10 shows the phase-difference between the corresponding angles 30, 60, 90, 120 and 150 degrees from the stagnation point for fD/U (Strouhal no) below 0.75 (Cases 0 and 3).

A simple calculation procedure using these phase-differences and the rms-pressure coefficients (weighted by an estimation of the coherence between the corresponding angles) in different Strouhal bands gave an estimation of the sectional pressure forces on the tube. The major contribution to the fluctuating lift came from energy around the fundamental Strouhal frequency (f_S) while the contributions to the fluctuating drag were dominated by energies at low Strouhal numbers (fD/U < 0.1) and from energy around the second harmonic ($2 f_S$). A comparison between cases 0 and 3 ($Re_D = 2.7 \cdot 10^4$, Tu = 0.1, 1.3 %) is summarized in Table 3.

Table 3 Calculated fluctuating force coefficients and measured quantities for cases 0 and 3. Tu = turbulence intensity at α = 90 deg, 0.1 diameter above the tube surface.

Case	C_{p_m}'	$C_p'(90)$	C_{p_b}'	$-C_{p_b}$	Tu[%]	C_D'	C_L'
0	0.32	0.27	0.22	1.20	4.0	0.07	0.54
3	0.41	0.37	0.30	1.32	5.4	0.09	0.73

These variations are in accordance with the estimates just given. For instance, the variations in C_L' are very similar to the variations in $C_p'(90)$ and the turbulence at the shoulder. As judged from [23], the turbulence effect seems to be a reduction in the length of the formation region. The alterations in the base pressure coefficients clearly demonstrates that the wake flow is affected by the stream turbulence.

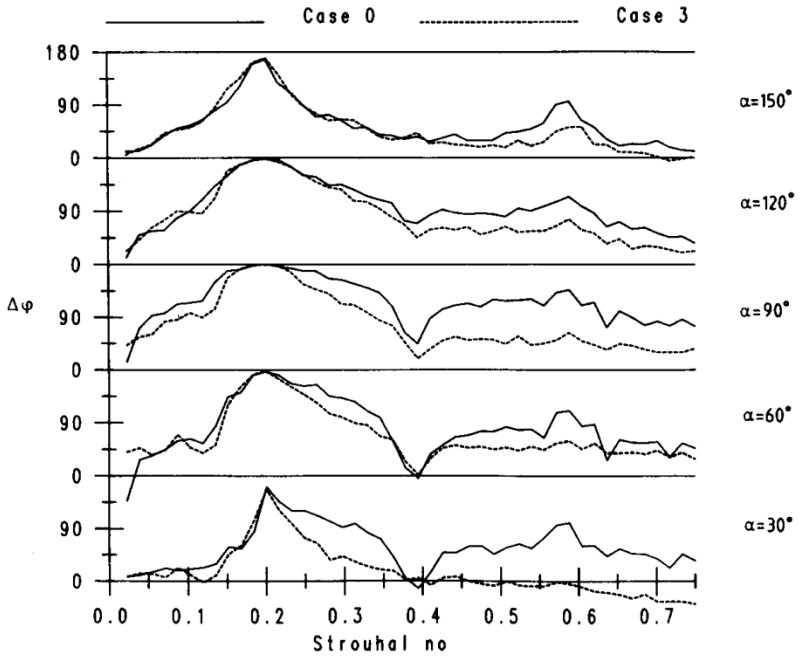

Fig. 10. Phase-difference between corresponding angles on the tube surfaces. Cases 0 and 3.

A more rigorous determination of C_L' and C_D' will be possible when the spanwise and circumferential correlation coefficients are available.

CONCLUSIONS

The results of the experimental investigation presented in this paper provide new and additional information concerning fluctuating pressures on a single tube placed in a turbulent stream.

The investigation was carried out at two different Reynolds numbers ($2.7 \cdot 10^4$ and $4.1 \cdot 10^4$) with varying turbulence intensity (0.1 - 3.2 %) and eddy size (Λ/D = 0.1 - 0.5) of the approaching stream.

For the flow ranges considered, the Reynolds number effect was small while the influence on the mean drag coefficient and maximum pressure coefficient by the stream turbulence was such that increases of order 5 % and 15 - 45 % occured, respectively, compared with the non-turbulent flow.

The experiments were all in the subcritical or pre-transitional range where the vortex shedding dominates the flow but an interaction between the stream turbulence and the vortex shedding was found.

Spectral and statistical analysis indicated that different physical mechanisms take place at various angular positions on the tube surface.

ACKNOWLEDGEMENTS

The present project is the Swedish contribution to the IEA - cooperative work on Heat Transfer and Heat Exchangers, Annex III Tube Vibration. The project is financially supported by the National Swedish Board for Technical Development.

REFERENCES

1. Owen, P.R., "Buffeting Excitation of Boiler Tube Vibration," J. Mech. Eng. Sci., Vol. 7, 1965, pp. 431-439.

2. So, R.M.C. and Savkar, S.D., "Buffeting Forces on Rigid Circular Cylinders in Cross Flows," J. Fluid Mech., Vol. 105, 1981, pp. 397-425.

3. Farell, C., "Flow around Fixed Circular Cylinders: Fluctuating Loads," J. Eng. Mech. Div., ASCE, Vol. 107, No. EM3, 1981, pp. 565-588.

4. Sunden, B., "A Theoretical Investigation of The Effect of Freestream Turbulence on Skin Friction and Heat Transfer for a Bluff Body," Int. J. Heat Mass Transfer, Vol. 22, No. 7, 1979, pp. 1125-1135.

5. Hanarp, L. and Sunden, B., "Structure of The Boundary Layers on a Circular Cylinder in the Presence of Freestream Turbulence," Lett. Heat Mass Transfer, Vol. 9, No. 3, 1982, pp. 169-177.

6. Hanarp, L. and Sunden, B., "An Investigation of the Influence of Freestream Turbulence on the Thermal Characteristics around a Single Tube," Symposium Series No. 86, I. Chem. Eng., Vol. 2, 1984, pp. 1125-1135.

7. Stansby, P.K., "The Effects of End Plates on the Base Pressure Coefficient of a Circular Cylinder," Aeronautical Journal, Vol. 78, Part 3, 1974, pp. 543-563.

8. West, G.S. and Apelt, C.J., "The Effects of Tunnel Blockage and Aspect Ratio on the Mean Flow Past a Circular Cylinder With Reynolds Number Between 10^4 and 10^5," J. Fluid Mech., Vol. 114, 1982, pp. 361-377.

9. Kiya, M., Suzuki, Y., Arie, M. and Hagino, M., "A Contribution to the Freestream Turbulence Effect on the Flow Past a Circular Cylinder," J. Fluid Mech., Vol. 115, 1982, pp. 151-164.

10. Arie, M., Kiya, M., Moriya, M. and Mori, H., "Pressure Fluctuations on the Surface of two Circular Cylinders in Tandem Arrangement," ASME J. Fluids Eng., Vol. 105, 1983, pp. 161-167.

11. Peterka, J.A. and Richardson, P.D., "Effects of Sound on Separated Flows," J. Fluid Mech., Vol. 37, Part 2, 1969, pp. 265-287.

12. Hatfield, H.M. and Morkovin, M.V., "Effect on an Oscillating Free Stream on the Unsteady Pressure on a Circular Cylinder," ASME J. Fluids Eng., Vol. 95, 1973, pp. 249-254.

13. Roshko, A., "Experiments on the Flow Past a Circular Cylinder at Very High Reynolds Number," J. Fluid Mech., Vol. 10, 1961, pp. 345-356.

14. Sadeh, W.Z. and Saharon, D.B., "Turbulence Effect on Crossflow around a Circular Cylinder at Subcritical Reynolds Number," NACA CR 3622, 1982.

15. Schlichting, H., Boundary Layer Theory, 7th ed., McGraw-Hill, New York, 1979.

16. Surry, D., "Some Effects of Intense Turbulence on the Aerodynamics of a Circular Cylinder at Subcritical Reynolds Number," J. Fluid Mech., Vol. 52, Part 3, 1972, pp. 543-563.

17. Igarashi, T., "Correlation Between Heat Transfer and Fluctuating Pressure in Separated Region of a Circular Cylinder," Int. J. Heat Mass Transfer, Vol. 27, No. 6, 1984, pp. 927-937.

18. Modi, V.J. and El-Sherbiny, S., "Effect of Wall Confinement on Aerodynamics of Stationary Cylinders," Proc. Wind Effects on Buildings and Structures, 1971, pp. 365-375.

19. Sonneville, P., "Etude de la Structure Tridimensionelle des Ecoulement Autour d'un Cylindre Circulaire," Bulletin de la Direction des Etudes et Recherches, Ser. A, No. 3, 1976, pp. 1-260.

20. Gerrard, J.H., "The Mechanisms of Formation Region of Vortices Behind Bluff Bodies," J. Fluid Mech., Vol. 25, No. 2, 1966, pp. 401-413.

21. Bloor, S., "The Transition to Turbulence in the Wake of a Circular Cylinder," J. Fluid Mech., Vol. 19, No. 2, 1964, pp. 290-304.

22. Gerrard, J.H., "An Experimental Investigation of the Oscillating Lift and Drag of a Circular Cylinder Shedding Turbulent Vortices," J. Fluid Mech., Vol. 11, 1961, pp. 244-256.

23. Gerrard, J.H., "A Disturbance-sensitive Reynolds Number Range of the Flow Past a Circular Cylinder," J. Fluid Mech., Vol. 22, No. 1, 1965, pp. 187-196.

reprinted from

Symposium on Flow-Induced Vibrations – Volume 1
Editors: M.P. Paidoussis, O.M. Griffin, and M. Sevik
(Book No. G00267)

published by

THE AMERICAN SOCIETY OF MECHANICAL ENGINEERS
345 East 47th Street, New York, N,Y, 10017
Printed in U.S.A.